



LIGO Laboratory / LIGO Scientific Collaboration

LIGO-T1000164-v4

ADVANCED LIGO

22 May 2020

Calculation and measurement of the OSEM actuator sweet spot position

Mark Barton

Distribution of this document:
DCC

This is an internal working note
of the LIGO Laboratory.

California Institute of Technology
LIGO Project – MS 18-34
1200 E. California Blvd.
Pasadena, CA 91125
Phone (626) 395-2129
Fax (626) 304-9834
E-mail: info@ligo.caltech.edu

Massachusetts Institute of Technology
LIGO Project – NW22-295
185 Albany St
Cambridge, MA 02139
Phone (617) 253-4824
Fax (617) 253-7014
E-mail: info@ligo.mit.edu

LIGO Hanford Observatory
P.O. Box 1970
Mail Stop S9-02
Richland WA 99352
Phone 509-372-8106
Fax 509-372-8137

LIGO Livingston Observatory
P.O. Box 940
Livingston, LA 70754
Phone 225-686-3100
Fax 225-686-7189

<http://www.ligo.caltech.edu/>

Table of Contents

1 Introduction..... 3
 1.1 Purpose and Scope 3
 1.2 References 3
 1.3 Version history, 3
2 Introduction..... 4
3 Theory..... 4
4 Measurement..... 10
 4.1 Results 13
5 Conclusions..... 15
6 Additional configurations..... 15

1 Introduction

1.1 Purpose and Scope

Several iterations of magnet holders and flags for the OSEMs have been designed according to a calculation in Mathematica by Mark Barton to put the working position of the magnet at the position of maximum force and minimum cross coupling to displacement of the OSEM. This report describes the calculation as well as measurements made to confirm it and check for any hard-to-model perturbations from ferromagnetic “plugs” used in the flags to allow snap-on functionality.

1.2 References

[T000119-00](#) - Use of magnets in the suspension design, Mark Barton.

[T060157-01](#), Review of the requirement for a reaction chain on the BS and FM suspensions in Advanced LIGO, Ken Strain

[M0900034-v3](#), Magnet sizes and types and OSEM types in Adv. LIGO suspensions

[D060401-G](#), Magnetic plug (Quad Noise Prototype)

[D060392-H](#), Magnet retainer (long type, for Quad Noise Prototype UI Mass)

[D060418-H](#), Magnet retainer (short type, for Quad Noise Prototype Top Mass)

[D060400-G](#), OSEM Magnet Flag (Quad Noise Prototype)

[D0901344](#), 10 mm diameter x 10 mm magnet

[D060218-C](#), Birmingham OSEM (BOSEM) assembly

[D060106-C](#), BOSEM coil former

[D0901065-v1](#), Value-engineered iLIGO OSEM (AOSEM) assembly

[D0901048-v4](#), AOSEM coil former

1.3 Version history,

3/26/10: Pre-rev-v1 draft.

4/1/10: Another draft, with lots more content.

4/5/10: Mostly complete -v1 draft, circulated to Norna for comment.

4/14/10: v1, based on better quality data taken 4/9 and 4/12, and with Norna’s feedback (new diagram, labeling of photo, discussion of implications, etc). Changed title to mention calculation.

4/29/10: v2, with calculations for paired magnets based on data from Joe.

5/3/10: v3, with fixes for errata noted by Bram, and new results for magnets to be used on tiptilts ($\varnothing 5 \times 10$).

5/22/20: v4, with fix for coupling issue noted by Norna.

2 Introduction

All of the various designs of OSEMs using in LIGO incorporate an actuator and a shadow sensor. The shadow sensor has a preferred working position for the object that interrupts the beam (either the magnet or a flag attached thereto) relative to the LED/PD which puts the sensor in the middle of the linear range. Similarly, the actuator has a preferred working position for the magnet relative to the coil which maximizes the force and minimizes the coupling from displacement of the object on which the OSEM is mounted. The position of the LED/PD relative to the coil and the length of any flag have to be chosen to ensure that both operating conditions are achieved simultaneously.

For some time the optimization of the actuator for different magnet/coil combinations has been done according to a calculation by Mark Barton not previously published but outlined in the theory section below. Early versions of this calculation assumed a simple dipole for the magnet which was probably adequate for the tiny iLIGO magnets. For the larger 10 mm diameter by 10 mm long magnets used on the quad the calculation was extended to integrate the force over both the volume of the coil and the volume of the magnet. However it wasn't updated to include the ferromagnetic disks introduced to implement snap-on functionality in the magnet holders and flags. And when the calculation needed to be revisited for the 5 mm long magnets used on the HSTS, additional confusion was encountered, with some hardware designs assuming out-of-date values for the coil dimensions.

This prompted a review of all the calculations plus an effort to confirm them with an experimental test.

3 Theory

The theory for the force on a current line element in a magnetic field is derived in the Mathematica notebook `MagDipole.nb` accompanying this document in the DCC. Briefly, if the magnitude and coordinates of a current element within the coil are

```
sourcecurrent = {j1x, j1y, j1z};
sourcepos = {dx, dy, dz};
```

and the coordinates of an arbitrary test point are (in the conventions of Mathematica's `Calculus`VectorAnalysis` package)

```
Coordinates[]
{Xx, Yy, Zz}
```

then the distance between them is

```
sourcefieldvec = Coordinates[]-sourcepos;
rsf = Sqrt[DotProduct[sourcefieldvec,sourcefieldvec]]
```

and the magnetic vector potential from the line element is

$$\mathbf{currentA} = \mu_0 / (4 \pi) \mathbf{sourcecurrent} / r_{sf}$$

$$\left\{ \begin{array}{l} \frac{j_{1x} \mu_0}{4 \pi \sqrt{(-dx + Xx)^2 + (-dy + Yy)^2 + (-dz + Zz)^2}}, \\ \frac{j_{1y} \mu_0}{4 \pi \sqrt{(-dx + Xx)^2 + (-dy + Yy)^2 + (-dz + Zz)^2}}, \\ \frac{j_{1z} \mu_0}{4 \pi \sqrt{(-dx + Xx)^2 + (-dy + Yy)^2 + (-dz + Zz)^2}} \end{array} \right\}$$

giving a field of

$$\mathbf{currentB} = \mu_0 / (4 \pi) \mathbf{Curl}[\mathbf{sourcecurrent} / r_{sf}]$$

$$\left\{ \begin{array}{l} \frac{\mu_0 \left(-\frac{j_{1z} (-dy + Yy)}{\left((-dx + Xx)^2 + (-dy + Yy)^2 + (-dz + Zz)^2 \right)^{3/2}} + \frac{j_{1y} (-dz + Zz)}{\left((-dx + Xx)^2 + (-dy + Yy)^2 + (-dz + Zz)^2 \right)^{3/2}} \right)}{4 \pi}, \\ \frac{\mu_0 \left(\frac{j_{1z} (-dx + Xx)}{\left((-dx + Xx)^2 + (-dy + Yy)^2 + (-dz + Zz)^2 \right)^{3/2}} - \frac{j_{1x} (-dz + Zz)}{\left((-dx + Xx)^2 + (-dy + Yy)^2 + (-dz + Zz)^2 \right)^{3/2}} \right)}{4 \pi}, \\ \frac{\mu_0 \left(-\frac{j_{1y} (-dx + Xx)}{\left((-dx + Xx)^2 + (-dy + Yy)^2 + (-dz + Zz)^2 \right)^{3/2}} + \frac{j_{1x} (-dy + Yy)}{\left((-dx + Xx)^2 + (-dy + Yy)^2 + (-dz + Zz)^2 \right)^{3/2}} \right)}{4 \pi} \end{array} \right\}$$

The field gradient is

$$\mathbf{currentgradB} = \mathbf{Grad}[\mathbf{currentB}]$$

$$\left\{ \left\{ \frac{\mu_0 \left(\frac{3 j_{1z} (-dx+Xx) (-dy+Yy)}{\left((-dx+Xx)^2 + (-dy+Yy)^2 + (-dz+Zz)^2 \right)^{5/2}} - \frac{3 j_{1y} (-dx+Xx) (-dz+Zz)}{\left((-dx+Xx)^2 + (-dy+Yy)^2 + (-dz+Zz)^2 \right)^{5/2}} \right)}{4 \pi}, \right. \\ \left. \frac{1}{4 \pi} \left(\mu_0 \left(\frac{3 j_{1z} (-dy+Yy)^2}{\left((-dx+Xx)^2 + (-dy+Yy)^2 + (-dz+Zz)^2 \right)^{5/2}} - \frac{3 j_{1y} (-dy+Yy) (-dz+Zz)}{\left((-dx+Xx)^2 + (-dy+Yy)^2 + (-dz+Zz)^2 \right)^{5/2}} - \frac{j_{1z}}{\left((-dx+Xx)^2 + (-dy+Yy)^2 + (-dz+Zz)^2 \right)^{3/2}} \right) \right), \\ \frac{1}{4 \pi} \left(\mu_0 \left(\frac{3 j_{1z} (-dy+Yy) (-dz+Zz)}{\left((-dx+Xx)^2 + (-dy+Yy)^2 + (-dz+Zz)^2 \right)^{5/2}} - \frac{3 j_{1y} (-dz+Zz)^2}{\left((-dx+Xx)^2 + (-dy+Yy)^2 + (-dz+Zz)^2 \right)^{5/2}} + \frac{j_{1y}}{\left((-dx+Xx)^2 + (-dy+Yy)^2 + (-dz+Zz)^2 \right)^{3/2}} \right) \right), \\ \left. \left\{ \frac{1}{4 \pi} \left(\mu_0 \left(-\frac{3 j_{1z} (-dx+Xx)^2}{\left((-dx+Xx)^2 + (-dy+Yy)^2 + (-dz+Zz)^2 \right)^{5/2}} + \frac{3 j_{1x} (-dx+Xx) (-dz+Zz)}{\left((-dx+Xx)^2 + (-dy+Yy)^2 + (-dz+Zz)^2 \right)^{5/2}} + \frac{j_{1z}}{\left((-dx+Xx)^2 + (-dy+Yy)^2 + (-dz+Zz)^2 \right)^{3/2}} \right) \right), \right. \\ \left. \frac{\mu_0 \left(-\frac{3 j_{1z} (-dx+Xx) (-dy+Yy)}{\left((-dx+Xx)^2 + (-dy+Yy)^2 + (-dz+Zz)^2 \right)^{5/2}} + \frac{3 j_{1x} (-dy+Yy) (-dz+Zz)}{\left((-dx+Xx)^2 + (-dy+Yy)^2 + (-dz+Zz)^2 \right)^{5/2}} \right)}{4 \pi}, \right. \\ \left. \frac{1}{4 \pi} \left(\mu_0 \left(-\frac{3 j_{1z} (-dx+Xx) (-dz+Zz)}{\left((-dx+Xx)^2 + (-dy+Yy)^2 + (-dz+Zz)^2 \right)^{5/2}} + \frac{3 j_{1x} (-dz+Zz)^2}{\left((-dx+Xx)^2 + (-dy+Yy)^2 + (-dz+Zz)^2 \right)^{5/2}} - \frac{j_{1x}}{\left((-dx+Xx)^2 + (-dy+Yy)^2 + (-dz+Zz)^2 \right)^{3/2}} \right) \right), \\ \left. \left\{ \frac{1}{4 \pi} \left(\mu_0 \left(\frac{3 j_{1y} (-dx+Xx)^2}{\left((-dx+Xx)^2 + (-dy+Yy)^2 + (-dz+Zz)^2 \right)^{5/2}} - \frac{3 j_{1x} (-dx+Xx) (-dy+Yy)}{\left((-dx+Xx)^2 + (-dy+Yy)^2 + (-dz+Zz)^2 \right)^{5/2}} - \frac{j_{1y}}{\left((-dx+Xx)^2 + (-dy+Yy)^2 + (-dz+Zz)^2 \right)^{3/2}} \right) \right), \right. \\ \left. \frac{1}{4 \pi} \left(\mu_0 \left(\frac{3 j_{1y} (-dx+Xx) (-dy+Yy)}{\left((-dx+Xx)^2 + (-dy+Yy)^2 + (-dz+Zz)^2 \right)^{5/2}} - \frac{3 j_{1x} (-dy+Yy)^2}{\left((-dx+Xx)^2 + (-dy+Yy)^2 + (-dz+Zz)^2 \right)^{5/2}} + \frac{j_{1x}}{\left((-dx+Xx)^2 + (-dy+Yy)^2 + (-dz+Zz)^2 \right)^{3/2}} \right) \right), \\ \left. \frac{\mu_0 \left(\frac{3 j_{1y} (-dx+Xx) (-dz+Zz)}{\left((-dx+Xx)^2 + (-dy+Yy)^2 + (-dz+Zz)^2 \right)^{5/2}} - \frac{3 j_{1x} (-dy+Yy) (-dz+Zz)}{\left((-dx+Xx)^2 + (-dy+Yy)^2 + (-dz+Zz)^2 \right)^{5/2}} \right)}{4 \pi} \right\} \right\}$$

The potential of a dipole element $\{m_2x, m_2y, m_2z\}$ in the field is

$$\mathbf{currentdipolepot} = \mathbf{currentB} \cdot \{m_2x, m_2y, m_2z\}$$

$$\begin{aligned} & \frac{m_2z \mu_0}{4\pi} \left(-\frac{j_1y (-dx+Xx)}{\left((-dx+Xx)^2 + (-dy+Yy)^2 + (-dz+Zz)^2\right)^{3/2}} + \frac{j_1x (-dy+Yy)}{\left((-dx+Xx)^2 + (-dy+Yy)^2 + (-dz+Zz)^2\right)^{3/2}} \right) + \\ & \frac{m_2y \mu_0}{4\pi} \left(\frac{j_1z (-dx+Xx)}{\left((-dx+Xx)^2 + (-dy+Yy)^2 + (-dz+Zz)^2\right)^{3/2}} - \frac{j_1x (-dz+Zz)}{\left((-dx+Xx)^2 + (-dy+Yy)^2 + (-dz+Zz)^2\right)^{3/2}} \right) + \\ & \frac{m_2x \mu_0}{4\pi} \left(-\frac{j_1z (-dy+Yy)}{\left((-dx+Xx)^2 + (-dy+Yy)^2 + (-dz+Zz)^2\right)^{3/2}} + \frac{j_1y (-dz+Zz)}{\left((-dx+Xx)^2 + (-dy+Yy)^2 + (-dz+Zz)^2\right)^{3/2}} \right) \end{aligned}$$

and the force on it is

$$\begin{aligned}
& \mathbf{currentdipoleforce} = -\mathbf{Grad}[\mathbf{currentB}.\{\mathbf{m2x},\mathbf{m2y},\mathbf{m2z}\}] \\
& \left\{ -\frac{m2x \mu_0 \left(\frac{3 j1z (-dx+Xx) (-dy+Yy)}{\left((-dx+Xx)^2 + (-dy+Yy)^2 + (-dz+Zz)^2 \right)^{5/2}} - \frac{3 j1y (-dx+Xx) (-dz+Zz)}{\left((-dx+Xx)^2 + (-dy+Yy)^2 + (-dz+Zz)^2 \right)^{5/2}} \right)}{4 \pi} \right. \\
& \frac{1}{4 \pi} \left(m2z \mu_0 \left(\frac{3 j1y (-dx+Xx)^2}{\left((-dx+Xx)^2 + (-dy+Yy)^2 + (-dz+Zz)^2 \right)^{5/2}} - \frac{3 j1x (-dx+Xx) (-dy+Yy)}{\left((-dx+Xx)^2 + (-dy+Yy)^2 + (-dz+Zz)^2 \right)^{5/2}} - \frac{j1y}{\left((-dx+Xx)^2 + (-dy+Yy)^2 + (-dz+Zz)^2 \right)^{3/2}} \right) \right) - \\
& \frac{1}{4 \pi} \left(m2y \mu_0 \left(-\frac{3 j1z (-dx+Xx)^2}{\left((-dx+Xx)^2 + (-dy+Yy)^2 + (-dz+Zz)^2 \right)^{5/2}} + \frac{3 j1x (-dx+Xx) (-dz+Zz)}{\left((-dx+Xx)^2 + (-dy+Yy)^2 + (-dz+Zz)^2 \right)^{5/2}} + \frac{j1z}{\left((-dx+Xx)^2 + (-dy+Yy)^2 + (-dz+Zz)^2 \right)^{3/2}} \right) \right), \\
& \left. \frac{m2y \mu_0 \left(-\frac{3 j1z (-dx+Xx) (-dy+Yy)}{\left((-dx+Xx)^2 + (-dy+Yy)^2 + (-dz+Zz)^2 \right)^{5/2}} + \frac{3 j1x (-dy+Yy) (-dz+Zz)}{\left((-dx+Xx)^2 + (-dy+Yy)^2 + (-dz+Zz)^2 \right)^{5/2}} \right)}{4 \pi} \right. \\
& \frac{1}{4 \pi} \left(m2z \mu_0 \left(\frac{3 j1y (-dx+Xx) (-dy+Yy)}{\left((-dx+Xx)^2 + (-dy+Yy)^2 + (-dz+Zz)^2 \right)^{5/2}} - \frac{3 j1x (-dy+Yy)^2}{\left((-dx+Xx)^2 + (-dy+Yy)^2 + (-dz+Zz)^2 \right)^{5/2}} + \frac{j1x}{\left((-dx+Xx)^2 + (-dy+Yy)^2 + (-dz+Zz)^2 \right)^{3/2}} \right) \right) - \\
& \frac{1}{4 \pi} \left(m2x \mu_0 \left(\frac{3 j1z (-dy+Yy)^2}{\left((-dx+Xx)^2 + (-dy+Yy)^2 + (-dz+Zz)^2 \right)^{5/2}} - \frac{3 j1y (-dy+Yy) (-dz+Zz)}{\left((-dx+Xx)^2 + (-dy+Yy)^2 + (-dz+Zz)^2 \right)^{5/2}} - \frac{j1z}{\left((-dx+Xx)^2 + (-dy+Yy)^2 + (-dz+Zz)^2 \right)^{3/2}} \right) \right), \\
& \left. \frac{m2z \mu_0 \left(\frac{3 j1y (-dx+Xx) (-dz+Zz)}{\left((-dx+Xx)^2 + (-dy+Yy)^2 + (-dz+Zz)^2 \right)^{5/2}} - \frac{3 j1x (-dy+Yy) (-dz+Zz)}{\left((-dx+Xx)^2 + (-dy+Yy)^2 + (-dz+Zz)^2 \right)^{5/2}} \right)}{4 \pi} \right. \\
& \frac{1}{4 \pi} \left(m2y \mu_0 \left(-\frac{3 j1z (-dx+Xx) (-dz+Zz)}{\left((-dx+Xx)^2 + (-dy+Yy)^2 + (-dz+Zz)^2 \right)^{5/2}} + \frac{3 j1x (-dz+Zz)^2}{\left((-dx+Xx)^2 + (-dy+Yy)^2 + (-dz+Zz)^2 \right)^{5/2}} - \frac{j1x}{\left((-dx+Xx)^2 + (-dy+Yy)^2 + (-dz+Zz)^2 \right)^{3/2}} \right) \right) - \\
& \frac{1}{4 \pi} \left(m2x \mu_0 \left(\frac{3 j1z (-dy+Yy) (-dz+Zz)}{\left((-dx+Xx)^2 + (-dy+Yy)^2 + (-dz+Zz)^2 \right)^{5/2}} - \frac{3 j1y (-dz+Zz)^2}{\left((-dx+Xx)^2 + (-dy+Yy)^2 + (-dz+Zz)^2 \right)^{5/2}} + \frac{j1y}{\left((-dx+Xx)^2 + (-dy+Yy)^2 + (-dz+Zz)^2 \right)^{3/2}} \right) \right) \left. \right\}
\end{aligned}$$

Because of cylindrical symmetry it is convenient to transform to cylindrical coordinates $\{r_1, \theta_1, z_1\}$ about the centre of the coil and $\{r_2, \theta_2, z_2\}$ about the centre of the magnet:

```
fdr1dr2dtheta1dtheta2dz1dz2 = (
  -r1*r2*currentdipoleforce
  /. dx -> r1*Cos[theta1]
  /. dy -> r1*Sin[theta1]
  /. dz -> z1
  /. j1x -> coilsigma*Sin[theta1]
  /. j1y -> -coilsigma*Cos[theta1]
  /. j1z -> 0
  /. Xx -> r2*Cos[theta2]
  /. Yy -> r2*Sin[theta2]
  /. Zz -> z2
  /. m2x -> 0
  /. m2y -> 0
  /. m2z -> mz
);
```

where `coilsigma` is the current density per unit area in the coil and `mz` is the magnetic moment per unit volume in the magnet.

Effectively, the above integrand is integrated over all six variables as follows:

```
force[z_] := Integrate[
  fdr1dr2dtheta1dtheta2dz1dz2,
  {z1, -coillen/2, coillen/2},
  {z2, z - 1/2, z + 1/2},
  {theta1, 0, 2 Pi},
  {theta2, 0, 2 Pi},
  {r1, coilrad1, coilrad2},
  {r2, 0, a}
]
```

where `coillen`, `coilrad1` and `coilrad2` are the coil length and inner and outer radii, `1` and `a` are the magnet length and radius, and `z` is the distance from the centre of the coil.

In practice, of the 6 integrations required, only `z1` and `z2` can be done analytically, or at least *could* in older versions of Mathematica. Newer versions of Mathematica seem to have gotten dumber but fortunately the results were archived because they took a long time to compute from scratch and are still available. See `SweetSpot.nb` for the expressions, which are too long to reproduce here.

The integrals over `theta1` and `theta2` can be combined by applying the transformation **`theta1 - theta2 -> deltatheta`**, and multiplying by `2*Pi`. The three remaining integrals, `deltatheta`, `r1` and `r2` can then be done numerically in a few seconds.

Table 1: Parameters for theoretical calculation and results - note mix of metric and customary units.

Parameter	5x10 magnet, BOSEM coil	10x10 magnet, BOSEM coil	5x10 magnet, old 400 turn coil	10x10 magnet, old 400 turn coil	Description
l	5 mm	10 mm	5 mm	10 mm	length of magnet
a	5 mm	5 mm	5 mm	5 mm	radius of magnet
coillen	0.315"	0.315"	0.16"	0.16"	length of coil
coilrad1	0.35"	0.35"	0.35"	0.35"	inner radius of coil
coilrad2	0.65"	0.65"	0.55"	0.55"	outer radius of coil
coilturns	800	800	400	400	number of turns
zflange	0.1"	0.1"			thickness of end flange
zplug	1 mm	1 mm			thickness of magnetic plug
mz (NdFeB)	$8.78 \cdot 10^5$	$8.78 \cdot 10^5$			magnetic moment/volume
coilsigma	$1.31 \cdot 10^7$ A/m ²	$1.31 \cdot 10^7$ A/m ²	$1.94 \cdot 10^7$ A/m ²	$1.94 \cdot 10^7$ A/m ²	coil current density
zc	10.04 mm	12.54 mm			calibration distance

4 Measurement

The OSEM force was measured as a function of magnet position for 5x10 and 10x10 magnets using the modal testing facility at Caltech.

A Newport NVM80 translation stage was laid on its side and clamped down, and the following items in order were bolted to it in a column (see photo in Figure 2 and diagram in):

- A ¼-20 to ¼-28 thread adapter.
- A Bruel and Kjaer 8230 force transducer.
- Another ¼-20 to ¼-28 adapter.
- A ¼-20 nut.
- A magnet retainer (D060392-H, long version, from UIM).
- A magnetic plug (D060401-G, pressed into the recess in the retainer).
- A magnet (10x10, D0901344, or 5x10)
- Another magnetic plug.

Using the long magnet retainer D060392-H with the 1½” shaft (as opposed to one with a short, 3/8” shaft, D060418) helped keep the magnet far from the force transducer to minimize possible interference from stray fields. The second magnetic plug was included for realism and was simply allowed to adhere magnetically to the magnet. In a real assembly it would previously have been pressed into an OSEM flag (D060400-G) but since the flag itself is non-magnetic and thus not expected to influence the sweet spot it was omitted for convenience.

A BOSEM (D060218-B) was bolted to a plate and held in the jaws of a vice clamped to the same base as the translation stage. By adjusting the plate in the jaws of the vice, the magnet could be centred in the aperture of the BOSEM. Initially however, the BOSEM was deliberately positioned about 1 cm to the side so that, when the stage was extended to bring the magnet in, the magnet butted against the face of the coil former. The reading on the translation stage micrometer when contact was made was recorded and used to relate subsequent readings to positions relative to the coil. Specifically, the distance of the centre of the magnet from the centre of the coil with the magnet in the butted position is

$$z_c \rightarrow l/2 + z_{\text{plug}} + z_{\text{flange}} + \text{coillen}/2$$

The magnet was then retracted, and the BOSEM was moved sideways in the jaws of the vice to be centred around the magnet as near as possible by eye.

The force transducer was plugged into the Bruel and Kjaer system as usual, and the OSEM coil was connected to the power amplifier that usually runs the shaker. The Bruel and Kjaer PULSE software was put into the mode normally used for calibrating the shaker. If the coil current is resistance limited, the expected transfer function is flat, and preliminary investigations revealed that this was indeed the case from a few Hz to around 60 Hz, limited by a rolloff in the force transducer at the low end and a resonance in the OSEM bracket at the upper end. Excitation was set to Periodic Random with 4 periods, which gave data with less scatter than Random or Pseudo Random. The excitation and analysis frequency ranges were set to 0-50 Hz with 100 lines of resolution. The power amplifier was set to its maximum gain and according to the meter on the front, a typical average voltage was 7.9 volts, which for a 38.4 ohm coil implies a current of 206 mA. However due to lack of time, that was the extent of the effort spent on amplitude calibration. The FFT value at 20 Hz was read using the cursor and recorded as representative of the flat function.

Figure 1: Diagram of experimental setup, with magnet at reference position (end plug in line with end flange)

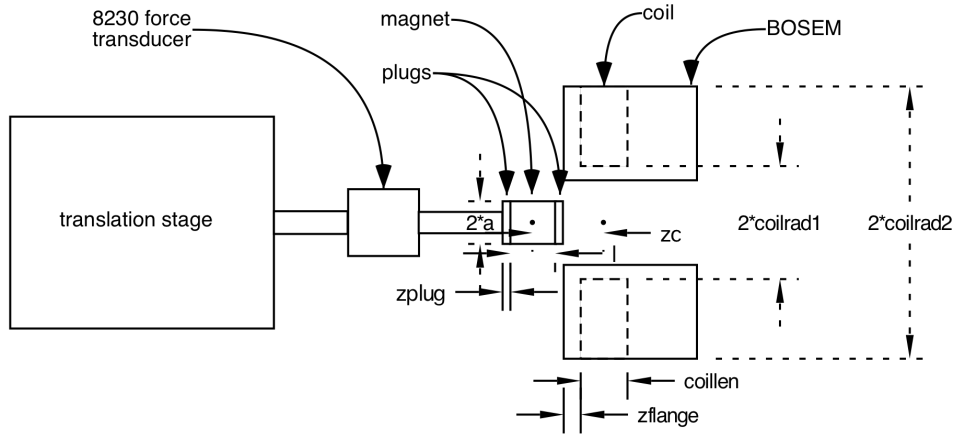
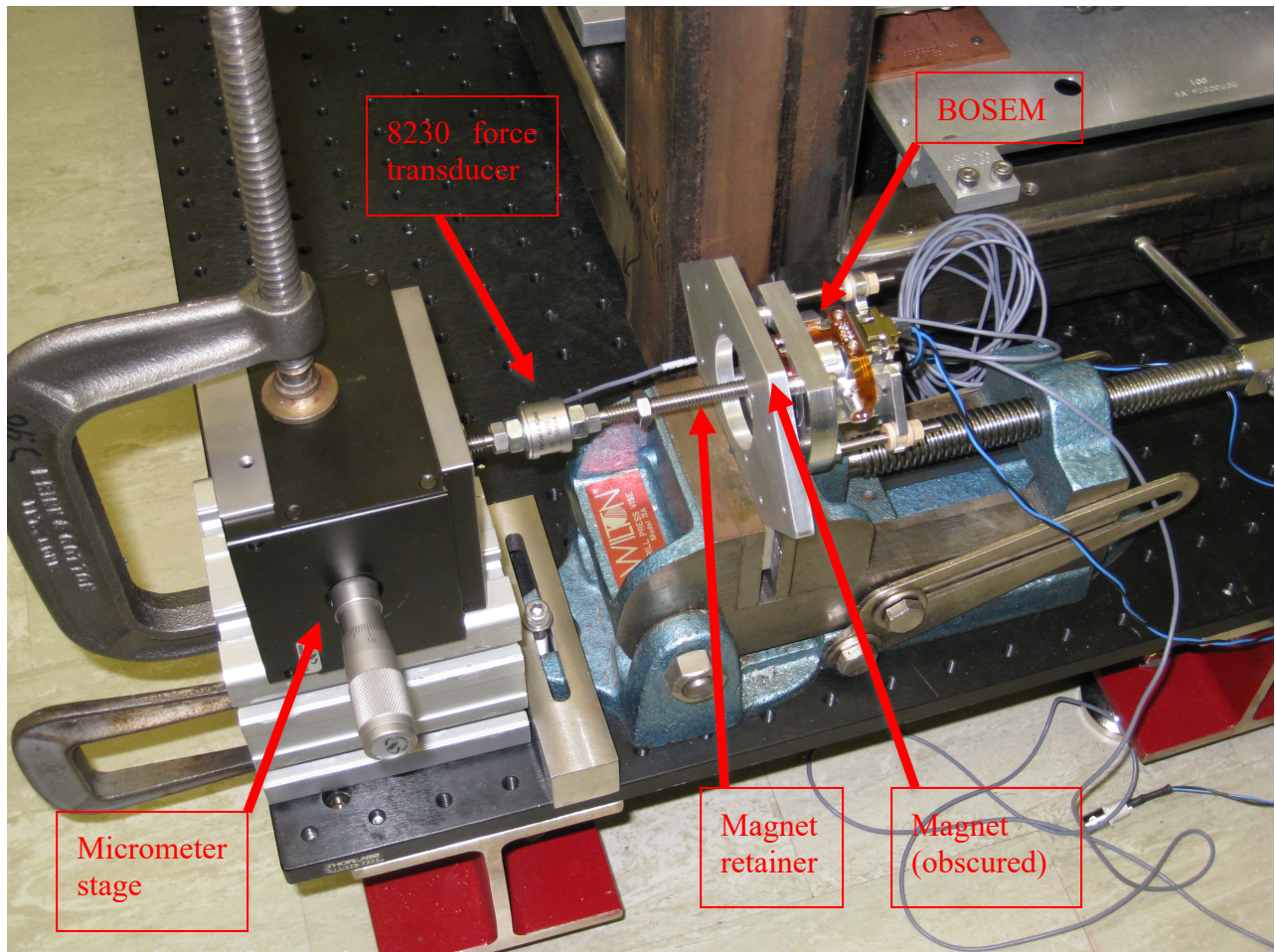


Figure 2: Experimental arrangement



4.1 Results

The data for the 10x10 NdFeB magnets is plotted in blue in Figure 3 as a function of distance from the centre of the coil, together with the theoretical predictions (ignoring any effect from the magnetic plugs) in black. Because an absolute calibration for the force was not available, the measured data has been scaled to have the same maximum as the theoretical curve. The subsequent agreement on other features of the curve is quite heartening but there is a slight offset in the position of the maximum. To quantify the discrepancy, the data in the symmetrical section immediately around the peak was fitted to a quadratic curve (plotted in red). The peak of the fitted curve is 0.15 mm further from the centre of the coil than predicted.

The data for the 5x10 magnets is plotted in Figure 4 with the same analysis as for the 10x10. Again, the agreement is quite heartening. The magnitude of the discrepancy is even smaller (0.03 mm) but the sign is opposite.

The results for both coils are summarized in Table 2.

Figure 3: Data for 10x10 magnet (blue) scaled to have same maximum value as theoretical prediction (black) with quadratic fit to central section (red).

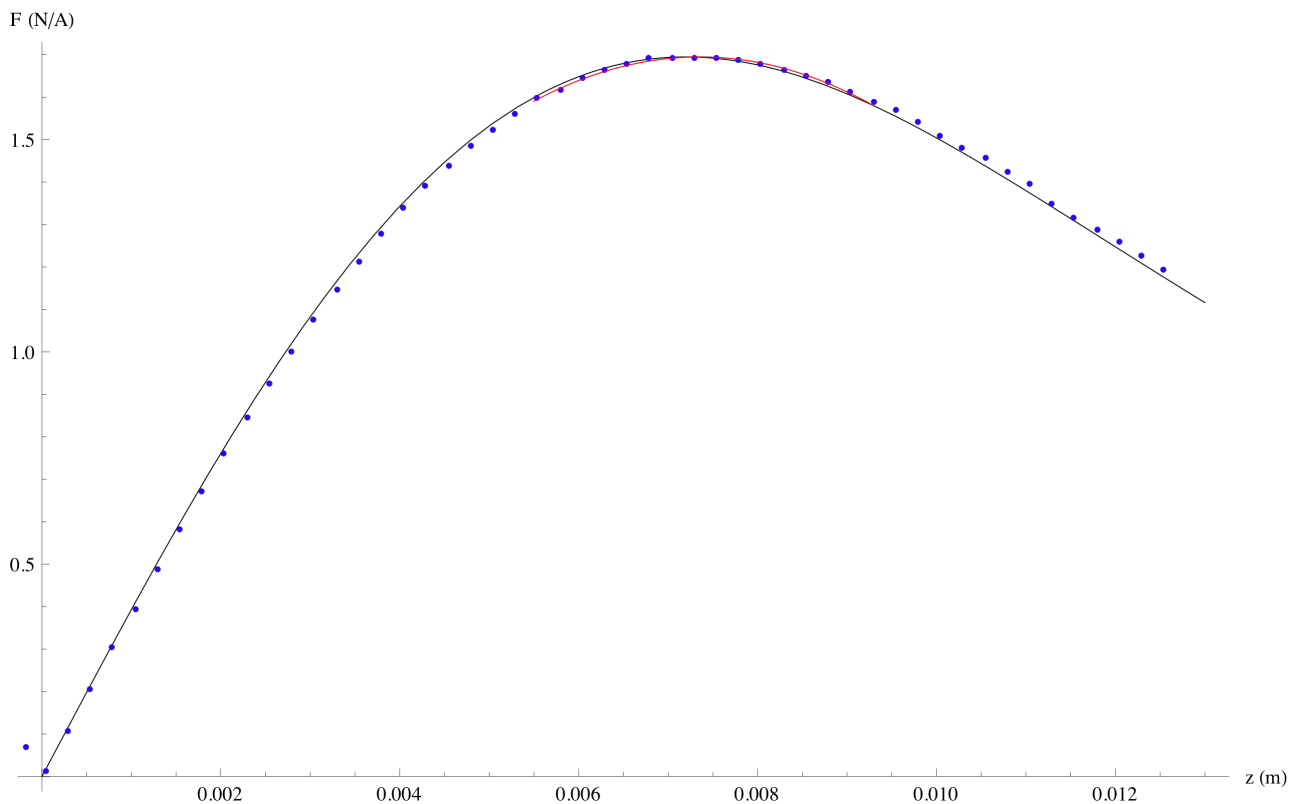


Figure 4: Data for 5x10 magnet (blue) scaled to have same maximum value as theoretical prediction (black) with quadratic fit to central section (red).

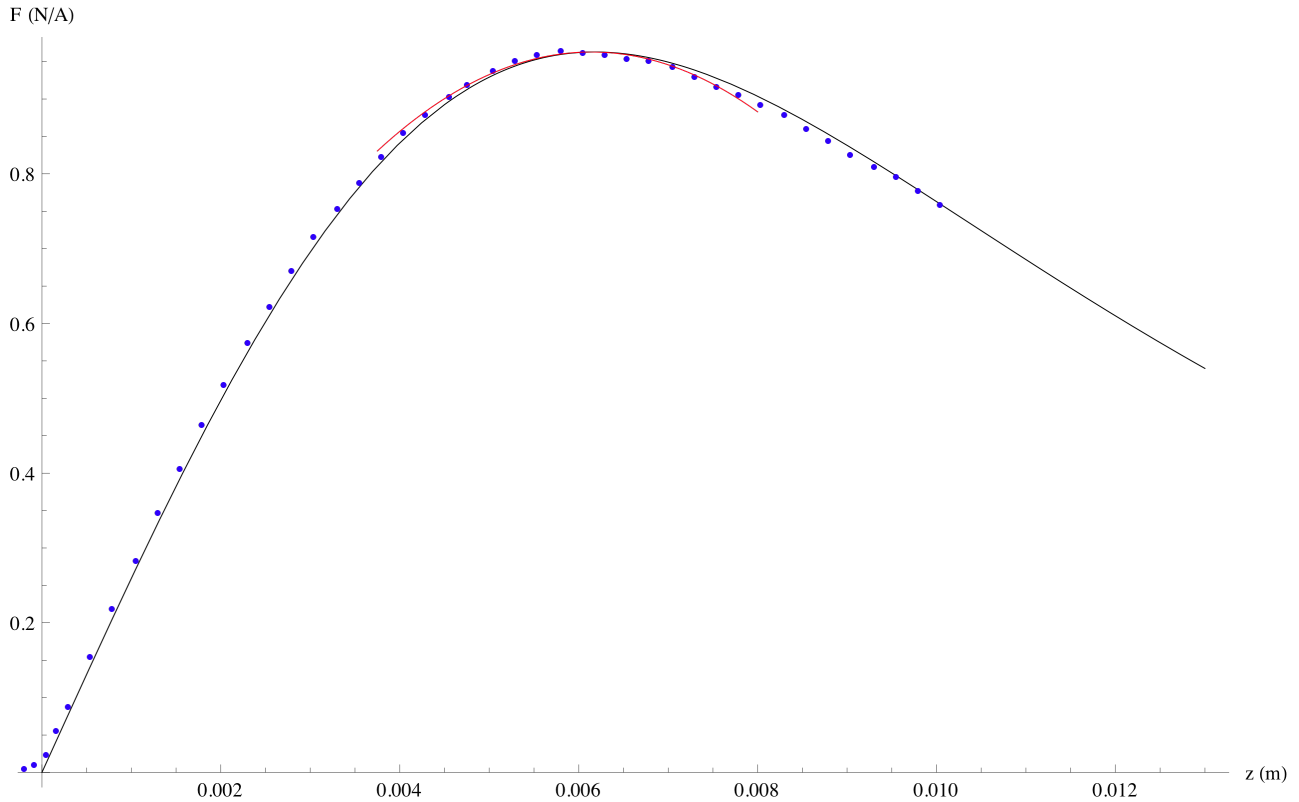


Table 2: Comparison of theoretical and measured results.

Parameter	5x10 magnet, BOSEM coil	10x10 magnet, BOSEM coil	5x10 magnet, old 400 turn coil	10x10 magnet, old 400 turn coil	Description
f_{\max} (theory)	0.963 N/A	1.694 N/A	0.637 N/A	1.08 N/A	maximum force (theory)
z_{\max} (theory)	6.18 mm	7.20 mm	5.09 mm	6.36 mm	sweet spot (theory)
$z_{\max q}$ (measured)	6.14 mm	7.35 mm			sweet spot (measured)
delta	-0.03 mm	0.16 mm			measured - theory
coupling (theory)	43.7 N/A/mm	195 N/A/mm	38.8 N/A/mm	73.7 N/A/mm	displacement-force cross-coupling

5 Conclusions

The agreement between theory and experiment is ± 0.21 mm, which is consistent with likely errors in relating the position of the centre of the coil to the position of the magnet when butted into the face of the coil. Any offset due to the magnetic plugs is either smaller than 0.2 mm or compensating for some other error.

If flag design cannot be delayed in the meantime, the best advice is probably to design to the theoretical values, i.e., 7.20 mm from the centre of the coil to the centre to the magnet for the 10x10 magnets and 6.18 mm for the 5x10. Note that this is for the -B version of the BOSEM which has an 800-turn, 0.315" coil (double that of pre-2006 versions).

If magnet flags have been designed to an out-of-date coil specification (such as the old 400 turn coil used on the hybrid OSEMs for the quad controls prototype) then there are two possible issues. First, if the OSEM is operated with the tip of the magnet or flag centred on the shadow sensor, the force will be slightly less than optimum. However the sweetspot is quite broad and it is very unlikely to be worth remaking parts to better optimize the force. For example, for the 10x10 magnet and the BOSEM coil, the peak force is at 7.20 mm but 95% or more of peak force is attained in the range 5.60 to 8.98 mm. A flag for a 400 turn hybrid OSEM coil used with an 800 turn BOSEM coil would put the magnet at 6.36 mm (see Table 2), which is well within this range.

Second, if there is a DC current in the coil there will be a noise force due to cross-coupling from displacement of the OSEM to applied force, which is zero at the position of peak force but increases linearly away from the optimum. Ken Strain calculated this for the BS suspension (T060157-01) and found that it was likely to be negligible because magnets at the upper mass were far enough away in the chain that any noise force would be sufficiently attenuated, and magnets at the intermediate mass would not have a DC current in the coils. Similar arguments are likely to apply for the quad. To facilitate the necessary calculations, the cross-coupling factors (the second derivatives of the force) have been given in the tables. **Note: -v3 had wildly wrong values here because it turns out that the numerical derivative function in Mathematica was not reliable when applied to multi-dimensional numeric integrals. A more reliable calculation using `FunctionInterpolation[]` to create a smooth approximation, and `Series[]` to extract the second derivative has been implemented. Norna Robertson attached a pre-release version of the -v4 calculation to the -v3 DCC document. The only significant change in the final -v4 version of the Mathematica is that the symbol name has been changed back to `coupling` to match the tables in this Word document – during debugging it had been `deriv2`.**

6 Additional configurations

The value-engineered LIGO-I style OSEMs (a.k.a. AOSEMs) will be used both with LIGO-I style magnets, and two other magnet sizes per M0900034. Coil and magnet data and calculated results for these configurations are given in Table 3.

In the quad, magnets are used in opposed pairs in several places to give a zero net dipole and thus reduced coupling to ambient magnetic fields. On the top mass and UIM, BOSEMs are used with pairs of $\varnothing 10 \times 10$ mm magnets with 20 mm between faces, and on the penultimate mass, AOSEMs are used with $\varnothing 2 \times 6$ mm magnets with 24 mm between faces. In each case the coil acts primarily on the near magnet, but there is a small effect on the far magnet which very slightly reduces the maximum force and coupling and very slightly increases the sweet spot distance (measured to the

centre of the near magnet). Values for these combinations are given in Table 4. The offset is only 0.1 mm for the $\varnothing 10 \times 10$ mm and 0.04 mm for the $\varnothing 2 \times 6$ mm, which is negligible.

Table 3: Parameters for theoretical calculation of additional combinations.

Parameter	AOSEM coil, iLIGO magnet	AOSEM coil, 6 mm x $\varnothing 2$ mm magnet	AOSEM coil, 0.5 mm x $\varnothing 2$ mm magnet	BOSEM coil, 10 mm x $\varnothing 5$ mm magnet	Description
l	0.125"	6 mm	0.5 mm	10 mm	length of magnet
a	0.0375"	1 mm	1 mm	2.5 mm	radius of magnet
coillen	0.16"	0.16"	0.16"	0.315"	length of coil
coilrad1	0.304"	0.304"	0.304"	0.35"	inner radius of coil
coilrad2	0.498"	0.498"	0.498"	0.65"	outer radius of coil
coilturns	400	400	400	800	number of turns
mz (NdFeB)	$8.78 \cdot 10^5$	$8.78 \cdot 10^5$	$8.78 \cdot 10^5$	$8.78 \cdot 10^5$	magnetic moment/volume
coilsigma	$1.54 \cdot 10^7$ A/m ²	$1.54 \cdot 10^7$ A/m ²	$1.54 \cdot 10^7$ A/m ²	$1.31 \cdot 10^7$ A/m ²	coil current density
fmax	0.0158 N	0.0309 N/A	0.00281 N/A	0.393 N/A	maximum force (theory)
zmax	5.34 mm	5.71 mm	5.20 mm	7.60 mm	sweet spot (theory)
coupling	0.919 N/A/mm	2.84 N/A/mm	0.169 N/A/mm	12.4 N/A/mm	displacement-force cross-coupling (theory)

Table 4: Combinations with paired magnets (values for single magnets from Table 2 and Table 3 are included for comparison).

Parameter	BOSEM coil, 10x10 magnets		AOSEM coil, 6 mm x ϕ 2 mm magnets		Description
	single	pair	single	pair	
		30 mm		30 mm	distance between centres
		20 mm		24 mm	distance between faces
fmax	1.69 N/A	1.63 N/A	0.0309 N/A	0.0303 N/A	maximum force (theory)
zmax	7.20 mm	7.30 mm	5.71 mm	5.75 mm	sweet spot (theory)
coupling	61.0 N/A/mm	195 N/A/mm	1.80 N/A/mm	2.84 N/A/mm	displacement-force cross-coupling (theory)